

Article

A Wearable Prefrontal Cortex Oxygen Saturation Measurement System Based on Near Infrared Spectroscopy

Yi Han ^{1,2,†} , Qian Zhai ^{1,†} , Yinkai Yu ¹, Shuoyu Wang ²  and Tao Liu ^{1,*} 

¹ State Key Laboratory of Fluid Power and Mechatronic Systems, School of Mechanical Engineering, Zhejiang University, Hangzhou 310027, China; 258012g@gs.kochi-tech.ac.jp (Y.H.); 11825031@zju.edu.cn (Q.Z.); 21960582@zju.edu.cn (Y.Y.)

² Department of Intelligent Mechanical Systems Engineering, Kochi University of Technology, Kochi 782-8502, Japan; wang.shuoyu@kochi-tech.ac.jp

* Correspondence: liutao@zju.edu.cn; Tel.: +86-0571-87951314 (ext. 6221)

† These authors contributed equally to this work.

Abstract: The measurement of blood oxygen saturation in the prefrontal cortex (PFC), especially during sleep, is of great significance for clinical research. Herein, we present a wearable PFC oxygen saturation measurement system using dual-wavelength functional near-infrared spectroscopy. The system is well designed for user-friendly donning and has the advantages of comfort, convenience, portability, and affordability. The performance of the proposed system is investigated by the calibration and experimental results. The wearable system has demonstrated great potential to conduct the physiological monitoring of PFC, and it can be widely deployed in daily life.

Keywords: near infrared spectroscopy; wearable; portable; prefrontal cortex oxygen saturation



Citation: Han, Y.; Zhai, Q.; Yu, Y.; Wang, S.; Liu, T. A Wearable Prefrontal Cortex Oxygen Saturation Measurement System Based on Near Infrared Spectroscopy. *Electronics* **2022**, *11*, 1971. <https://doi.org/10.3390/electronics11131971>

Academic Editor: J.-C. Chiao

Received: 14 May 2022

Accepted: 15 June 2022

Published: 24 June 2022

Publisher's Note: MDPI stays neutral with regard to jurisdictional claims in published maps and institutional affiliations.



Copyright: © 2022 by the authors. Licensee MDPI, Basel, Switzerland. This article is an open access article distributed under the terms and conditions of the Creative Commons Attribution (CC BY) license (<https://creativecommons.org/licenses/by/4.0/>).

1. Introduction

The prefrontal cortex (PFC), responsible for complex thinking and decision-making, as well as emotional regulation, is fundamental to the physiological activities of humans [1]. Nightly sleep restores the brain and is correlated with physical repairs and memory consolidation. A sufficient and stable oxygen supply to cerebral cortex tissue is essential for the relaxation of the brain [2]. Several diseases cause various local microvascular or respiratory modifications, resulting in changes of tissue oxygen saturation [3,4]. Subtle alterations in sleep quality result in consequential next-day changes in emotion or intentness [5]. Therefore, the accurate measurement of blood oxygen saturation in the PFC tissue is of great significance for clinical research. In this way, physiological information can be acquired, and then corresponding effective treatments can be taken in time [6].

In the 1870s, Jobsis [7] first obtained blood oxygen changes and deep physiological information in the heads of animals through near infrared light. The absorption of light by the main absorbers (i.e., oxyhemoglobin (HbO_2) and deoxyhemoglobin (Hb)) in the blood varies with the oxygen saturation. Hence, the absorbed components of the light reflected from the human tissue can be analyzed to obtain the blood oxygen saturation [8]. With the advantages of portability, affordability, low susceptibility to noise, and moderate temporal resolution compared with the medical polysomnography (PSG) procedure, functional near-infrared spectroscopy (fNIRS) based technologies have attracted increasing attention [9]. Oniz et al. investigated the refreshing property of sleep in terms of sleep stages using fNIRS to measure PFC hemodynamics [10]. Nguyen et al. investigated the brain's functional connectivity in rest and sleep states using fNIRS [11]. Ahn et al. combined fNIRS with multimodal EEG/ECG/EOG data to quantify mental fatigue during performed simulated driving under two different conditions (well-rested and sleep-deprived) [12]. The previous research works have demonstrated that some of the activities and states during sleep are relevant to the blood oxygen changes of PFC. The fNIRS-based technologies enable the

non-invasive sensing of these physiological phenomena. Combined with other modalities, fNIRS can aid in characterizing and understanding the complex phenomena and be applied in sleep monitoring. Nevertheless, sleep disorders, such as obstructive sleep apnea, significantly deteriorate the cerebral oxygen supply to the brain. Little research has illuminated the effects of respiratory modifications during sleep using fNIRS. There are also some well-known commercial products, such as Somanetics INVOS [13], CASMED FOREE-SIGHT [14], Hamamatsu NIRO [15], and Shimadzu OM-100, which have been applied in clinical monitoring. These devices are complex, expensive, and restricted to hospitals. The past decade has witnessed an increasing expectation for in-home health management [16]. However, the fNIRS-based research on PFC physiology, especially during sleep, is primary, and the current measurement systems are not suitable for daily monitoring. To monitor the physiological activities of PFC continuously and conveniently, the aim of this research is to design a novel fNIRS-based wearable system, validate the performance of monitoring PFC oxygen saturation, and investigate its potential for sensing-related activities, especially during sleep. The system is miniaturized, user-friendly, affordable, and convenient for applications in non-hospital facilities.

The rest of the paper is organized as follows. In Section 2, the analytical model and the measurement system are presented in detail. Section 3 describes the experimental setup and protocols. In Section 4, the results are illustrated and discussed. Finally, a brief conclusion is drawn.

2. Measurement System Description

2.1. Analytical Model

Assuming that the absorption rate and scattering coefficient of biological tissue are constant, the blood oxygen saturation is highly relevant to the decay of light intensity due to the absorption of Hb and HbO_2 [17]. The modified Lambert–Beer law describes the quantitative relationship between the light absorption and the characteristics of the tissue:

$$B^\lambda = \log\left(\frac{I_0}{I}\right) = (\alpha_{HbO_2}^\lambda C_{HbO_2} + \alpha_{Hb}^\lambda C_{Hb}) \cdot DPF \cdot r + G, \quad (1)$$

where B is the attenuation of light intensity, I_0 and I are the incident light intensity and emitted light intensity, respectively, α is the absorption coefficient of the chromophores at a specific wavelength, λ is the wavelength of the light, C_{HbO_2} and C_{Hb} are the concentrations of HbO_2 and Hb , DPF denotes the differential path factor (e.g., 6.53 in our application [18]), r is the distance between light source–detector pairs, and G is a geometry-dependent factor representing the intensity loss caused by scattering. When the concentrations of HbO_2 and Hb change, the attenuation of light intensity changes homogeneously:

$$\Delta B^\lambda = \log\left(\frac{I_0}{I}\right) = (\alpha_{HbO_2}^\lambda \Delta C_{HbO_2} + \alpha_{Hb}^\lambda \Delta C_{Hb}) \cdot DPF \cdot r, \quad (2)$$

If the absorption changes are measured at two wavelengths, λ_1 and λ_2 , the concentration changes of HbO_2 and Hb can be computed as

$$\begin{aligned} \Delta C_{HbO_2} &= \frac{\Delta B^{\lambda_1} \alpha_{Hb}^{\lambda_2} - \Delta B^{\lambda_2} \alpha_{Hb}^{\lambda_1}}{DPF \cdot r \cdot (\alpha_{Hb}^{\lambda_2} \alpha_{HbO_2}^{\lambda_1} - \alpha_{Hb}^{\lambda_1} \alpha_{HbO_2}^{\lambda_2})}, \\ \Delta C_{Hb} &= \frac{\Delta B^{\lambda_1} \alpha_{HbO_2}^{\lambda_2} - \Delta B^{\lambda_2} \alpha_{HbO_2}^{\lambda_1}}{DPF \cdot r \cdot (\alpha_{Hb}^{\lambda_1} \alpha_{HbO_2}^{\lambda_2} - \alpha_{Hb}^{\lambda_2} \alpha_{HbO_2}^{\lambda_1})}. \end{aligned} \quad (3)$$

The blood oxygen saturation rSO_2 can be calculated as

$$rSO_2 = \frac{C_{HbO_2}}{C_{HbO_2} + C_{Hb}} = \frac{\alpha_{Hb}^{\lambda_1} - \alpha_{Hb}^{\lambda_2} \frac{B^{\lambda_1}}{B^{\lambda_2}}}{\frac{B^{\lambda_1}}{B^{\lambda_2}} (\alpha_{HbO_2}^{\lambda_2} - \alpha_{Hb}^{\lambda_2}) - (\alpha_{HbO_2}^{\lambda_1} - \alpha_{Hb}^{\lambda_1})}. \quad (4)$$

Since light with a wavelength longer than 900 nm is easily absorbed by water and light with a wavelength shorter than 700 nm is excessively absorbed by hemoglobin, the dual wavelengths of 760 nm and 850 nm are selected for measurement.

2.2. System Structure

The structure of the fNIRS-based measurement system is shown in Figure 1. The system consists of the micro-processor unit (MPU), infrared emission module, sampling module, Bluetooth transmission module, and graphical user interface (GUI). The infrared emission module is fixed to the forehead of subjects and controls the emission of near-infrared light. Then, the sampling module detects the intensity of the received light. Finally, the blood oxygen saturations at different positions in the PFC are calculated by the MPU. The results will be transmitted to the GUI via Bluetooth.

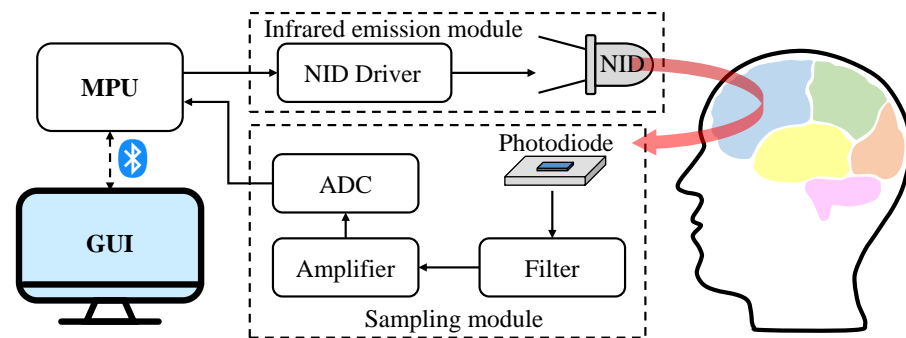


Figure 1. The schematic diagram of the designed system structure.

The infrared emission module consists of near-infrared diodes (NID) and an NID driver. In consideration of light intensity and penetration depth, the module utilizes the diodes (e.g., W760/850-O4L) that integrate sources of dual wavelengths (i.e., 760 nm and 850 nm). It has the advantages of a small size, low cost, and embedability. The MPU and the constant current driver (e.g., MBI5168) with multiple outputs control the emission timing of multiple NIDs. The sampling module consists of photodiodes, a filter, an amplifier, and an analog-to-digital-converter (ADC). The photodiodes (e.g., OPT101) receive the emitted near-infrared light and convert light signals into electrical signals. They have high sensitivity within the wavelength from 700 nm to 900 nm. Since the change of the PFC oxygen saturation is relatively low compared with external noises, low-pass filters are employed to eliminate high-frequency interference. Then, the filtered signals are magnified by the amplifier (e.g., AD623) and are converted into digital signals by the ADC channels. Moreover, we select STM32 for timing control and oxygen saturation calculation, HC-05 for Bluetooth transmission, and SPX3819 for power supply.

2.3. Wearable Design

Figure 2 illustrates the distribution of the NID and photodiodes in one probe module. One NID is placed in the center of four photodiodes, and the distance between each NID–photodiode pair is approximately 28 mm. Hence, the near-infrared light can transmit through the deeper tissue layers.

As shown in Figure 3, two probe modules are employed in the system, and the distance between the NIDs is approximately 60 mm. To minimize the interference resulting from the environment or movement, it is essential to block out the natural light from the detection area and ensure a tight connection between the sensor and the forehead. In each probe module, a baffle is fixed in the back as a shelter. The connection of probe modules adopts the hinge structure, and silicone is used for the contact between modules and forehead to better fit the various subjects and improve wearing comfort.

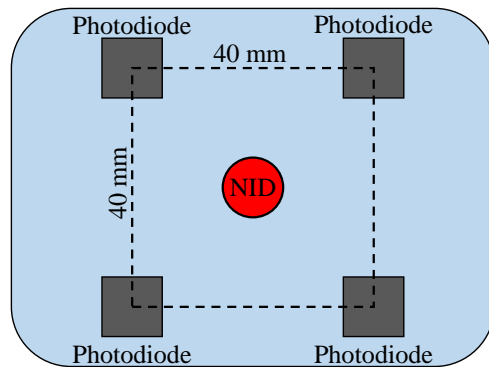


Figure 2. The distribution diagram of the probes.

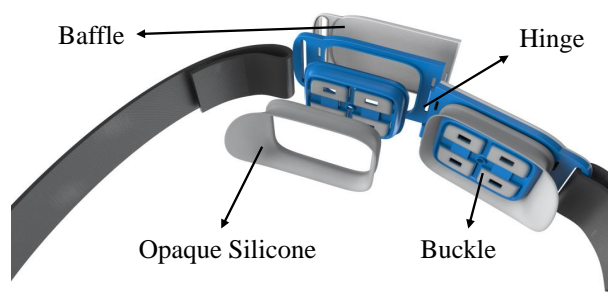


Figure 3. The wearable design of the measurement system.

3. Experiments

Firstly, the optical integrating sphere model as illustrated in Figure 4 is exploited to simulate human tissue [19]. The emitted near infrared light that transmits through the sphere model has the same optical power as the incident light. By adjusting the light filter, the model can imitate the attenuation effect of human tissue with a different oxygen saturation and realize the multi-point calibration of oxygen saturation measurement.

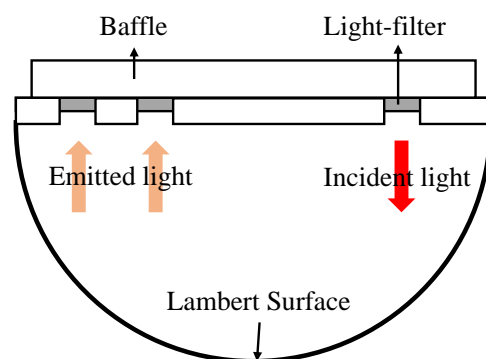


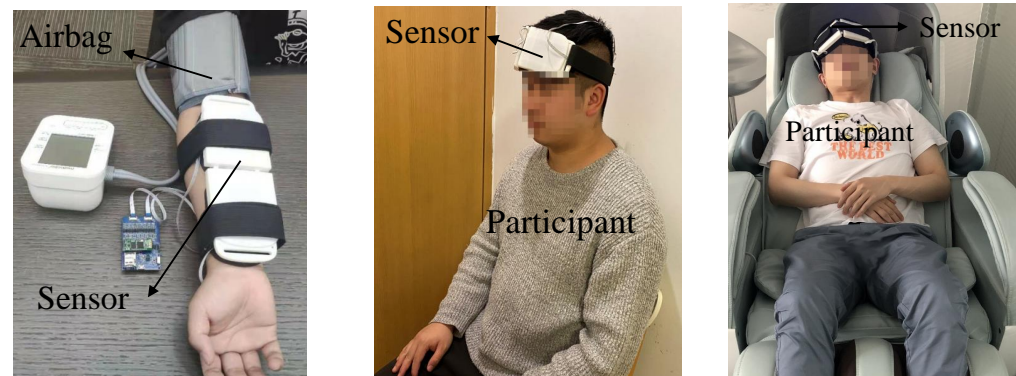
Figure 4. Diagram of the optical integrating sphere model.

In order to verify the performance and reliability of the system, a forearm arterial occlusion experiment, motor imagery experiment, and sleep experiment were performed. Participants aged from 20 to 25 years old were recruited for the experiments. The participants had no major diseases, and the blood pressure of each participant was normal and stable.

As shown in Figure 5a, each participant wore an inflatable airbag in the forearm arterial occlusion experiment. When the inflated airbag pressed the arm, the concentrations of HbO_2 and Hb changed correspondingly. The steps of the forearm arterial occlusion experiment were implemented as follows:

1. Let the participant sit upright in the chair and place his right arm parallel on the table;

2. Fix the measurement system to the front side of the arm and fix the airbag to the upper arm of the participant;
3. Turn on the measurement system when the participant relaxes;
4. Fifteen seconds later, inflate the airbag to press the upper arm;
5. Fifteen seconds later, release the airbag;
6. Turn off the measurement system.



(a) Forearm Block Experiment (b) Motor Imagery Experiment (c) Sleep Experiment

Figure 5. (a) Each participant wore the measurement system and an inflatable airbag on their arm in the forearm arterial occlusion experiment. (b) Each participant wore the measurement system on their forehead in the motor imagery experiment. (c) Each participant lay in a pod and wore the measurement system on their forehead in the sleep experiment.

The PFC is responsible for complex thinking and decision-making. The blood oxygen saturation of this brain region will change with physiological activities. To detect the movement intention, each participant wore the measurement system on their forehead, as shown in Figure 5b in the motor imagery experiment. The steps were implemented as follows:

1. Let the participant sit in the chair and fix the measurement system onto their forehead;
2. Turn on the system and let the participant close their eyes throughout the experiment;
3. Ten seconds later, ask the participant to imagine walking upstairs;
4. Forty seconds later, let the subject stop imagining and relax;
5. Turn off the measurement system.

Different biological processes through the sleep cycle probably affect breathing or the muscles. Deep breathing or sleep apnea will result in a change of the blood oxygen saturation in the PFC. As shown in Figure 5c, the participants lay in a nap pod and were asked to breathe normally, breathe deeply, and hold their breath. Clinical medical staffs were consulted to help subjects to conduct the experiments and record the events. The steps were implemented as follows:

1. Let the participant lie in the nap pod and fix the measurement system onto their forehead;
2. Turn on the system and let the participant close their eyes throughout the experiment;
3. Fifteen seconds later, ask the participant to breathe deeply or hold their breath;
4. Thirteen seconds later, let the subject breathe normally;
5. Turn off the measurement system.

4. Results

Figure 6 shows the calibration results where the triangles represent the measured values, the red line represents the ideal line, and the black line represents the fitted line. The measurement range of the oxygen saturation is between 0.5–0.75, which is the same as human tissue. The correlation coefficient between the fitted line and ideal line is about 0.98, and the result demonstrates the accuracy of the system.

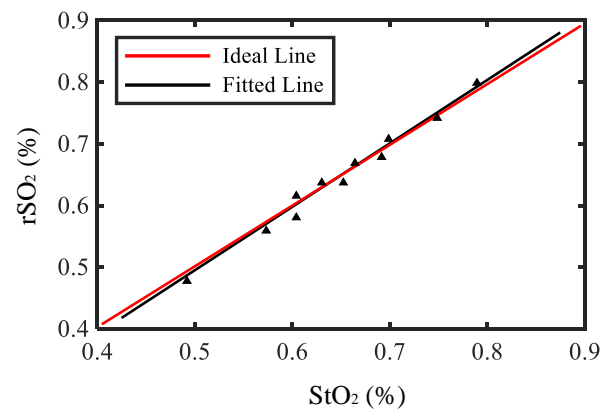


Figure 6. The calibration result of the system.

Figure 7 shows one example of the measurement result in the forearm arterial occlusion experiment. At the beginning, the concentrations of HbO_2 and Hb remained stable when the participant stayed relaxed. When the airbag was inflated and the forearm arterial was occluded, blood flow to the forearm was restricted as well as the oxygen. Hence, HbO_2 in the forearm was partially converted into Hb when the oxygen was consumed. Consistently, the measured concentration of HbO_2 increased and the concentration of Hb decreased in Figure 7. After the airbag was released, the two concentrations returned to the normal state.

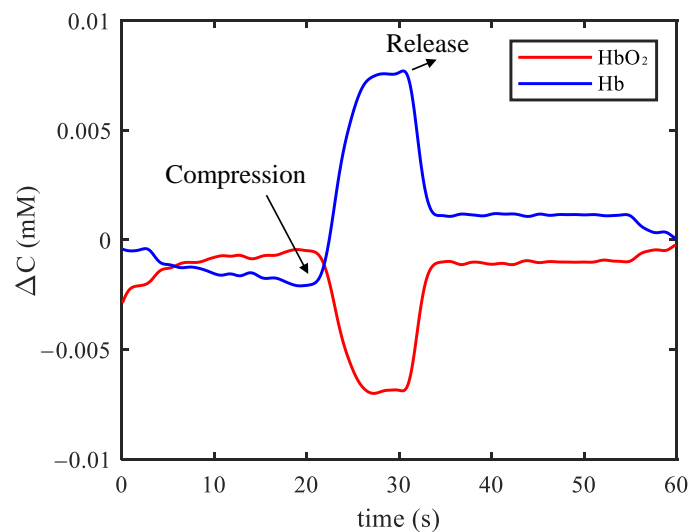


Figure 7. Example of results in the forearm arterial occlusion experiment.

Figure 8 shows one example of the measurement result in the motor imagery experiment. The concentrations of HbO_2 and Hb were unchanged in the relaxing condition. When the participant started to imagine walking upstairs, the blood flow in PFC and the transmission of oxygen increased. It is also illustrated as in Figure 8 that the concentration of HbO_2 increased sharply and the concentration of Hb also had a slight increase.

Figure 9a shows one example of the measurement result in the deep breath experiment. The deep breath improved the blood supply to the brain. When the participant started to breathe deeply, the concentration of HbO_2 increased rapidly and the concentration of Hb decreased. Finally, the concentrations returned to the normal level. Figure 9b shows one example of the measurement result in the apnea experiment. Holding breath increased the intrathoracic pressure, resulting in restricted blood flow. When the participant started to hold their breath, the concentration of HbO_2 decreased, and the concentration of Hb had a slight increase as shown in Figure 9c. When the participant breathed normally again, the concentrations slowly returned to the normal level.

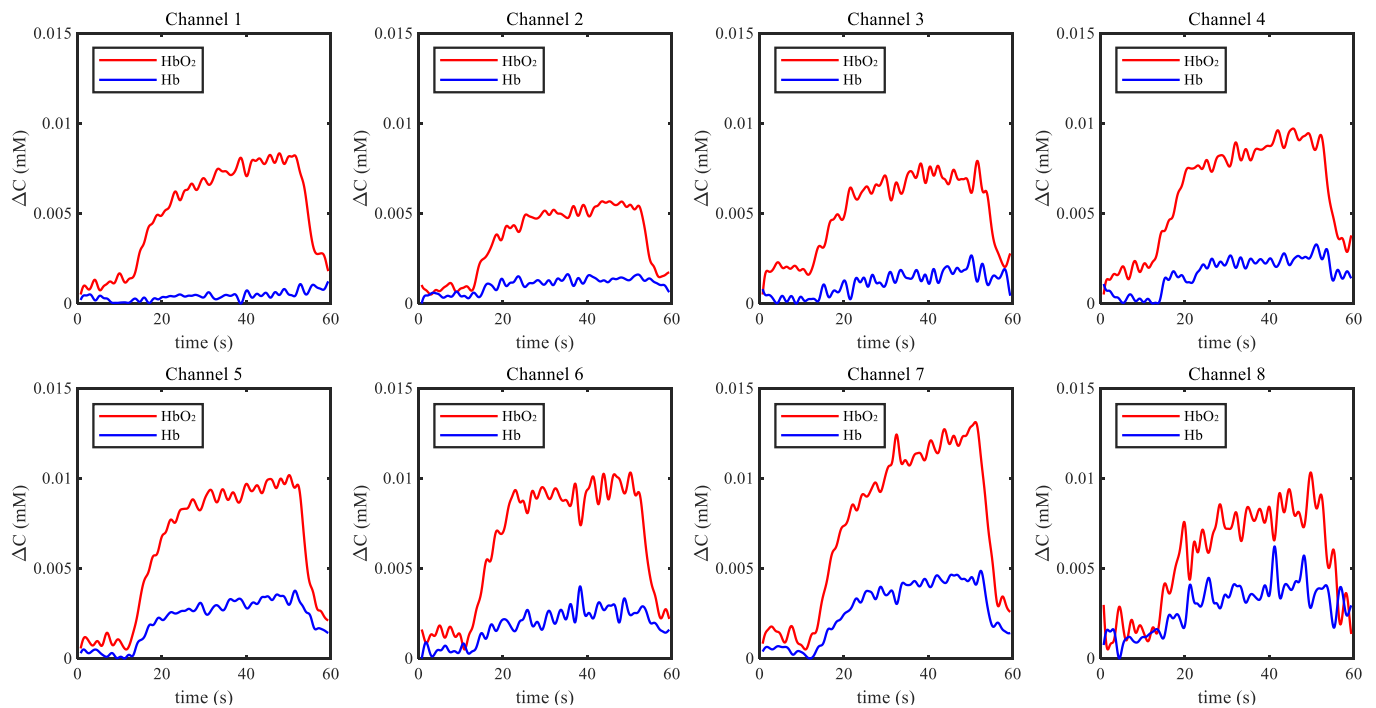
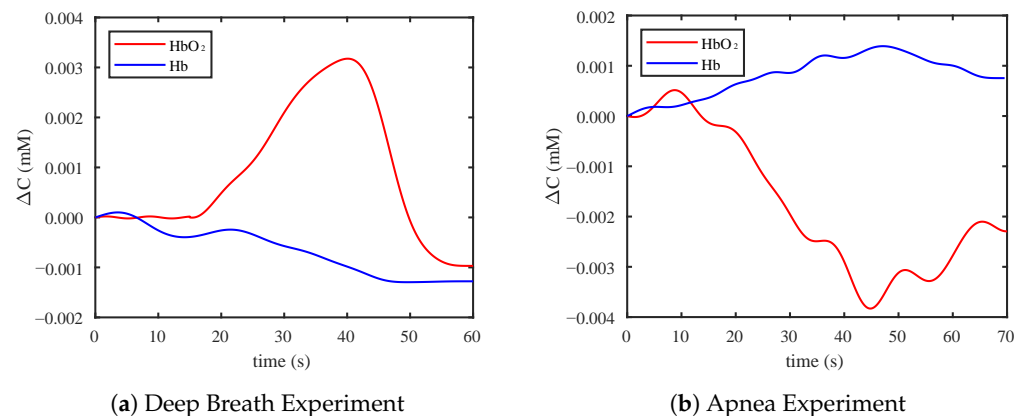


Figure 8. Example of results in the motor imagery experiment.



(a) Deep Breath Experiment

(b) Apnea Experiment

Figure 9. (a) Example of results in the deep breathing experiment. (b) Example of results in the apnea experiment.

5. Discussion

The calibration and experimental results demonstrate that the changes of the concentrations of HbO_2 and Hb in PFC can be measured accurately by the system. The correlation coefficient of 0.98 in the calibration is comparable with a coefficient larger than 0.95 in [8]. The physiological phenomenon in the forearm arterial occlusion experiment and motor imagery experiment are consistent with results in [8,20], respectively. The measurement system has dimensions of $17.5 \times 7 \times 3.5$ cm and weighs around 600 g, which is smaller and lighter compared with the system that has dimensions of $18.5 \times 7.5 \times 7$ cm and a weight of around 1200 g in [21]. Moreover, conventional near-infrared blood oxygen measurement devices have some disadvantages, such as a complex structure, large size, high cost, and wearing discomfort. The proposed sensor unit employs a hinge in its structure to enable adaptive deformation and soft silicone as a material for flexible contact with the forehead. With the miniaturization and lightweight design, the wearable system is comfortable, convenient, and not expensive. It has great potential to get rid of site restriction and be promoted to non-hospital facilities.

Currently, the proposed system also has some limitations. First, the system is verified based on healthy subjects only, and we do not focus on a specific population, such as

patients with sleep apnea. Second, the sensor units may generate pressure on the forehead to ensure the stable contact. Third, the human-computer interface and measurement region are preliminarily designed for non-clinical experimental tests. For future work, the software interface will be further optimized for clinical application. Then the system can be employed to implement experiments of patients and record over-night sleep events. We will explore methods to detect the physiological activities including sleep apnea.

6. Conclusions

A wearable PFC oxygen saturation measurement system based on fNIRS is proposed in this research. The system is comfortable, easy-to-use, portable, and low-cost. The performance of the wearable blood oxygen saturation measurement system is investigated by the calibration accuracy and experimental results. The changes of the hemoglobin concentrations in PFC can be measured accurately by the system. It is demonstrated that the proposed system has great potential to conduct the physiological monitoring of the PFC, and it can be widely deployed in non-hospital facilities and in daily life.

Author Contributions: Conceptualization, T.L. and S.W.; methodology, Y.H. and Y.Y.; software, Y.H. and Y.Y.; validation, Y.Y.; formal analysis, Q.Z.; investigation, Y.H. and Q.Z.; resources, T.L. and S.W.; data curation, Q.Z.; writing—original draft preparation, Q.Z.; writing—review and editing, Q.Z.; visualization, Y.Y.; supervision, T.L.; project administration, Y.H.; funding acquisition, T.L. All authors have read and agreed to the published version of the manuscript.

Funding: This research was funded in part by the NSFC Grant No. 52175033 and No. U21A20120, in part by Zhejiang Provincial Natural Science Foundation of China under Grant LZ20E050002, in part by Zhejiang Provincial Key Research and Development Program under Grant 2021C03051, 2021C03G2013248, and 2019C03080, and in part by Hangzhou Leading Innovation and Entrepreneurship Team under Grant 2018TD06.

Institutional Review Board Statement: The study was approved by the Medical Ethics Committee of Zhejiang Hospital (Approval Letter NO: AF/SC-06/04.2).

Conflicts of Interest: The authors declare no conflict of interest.

References

1. Leopold, D.; Phillips, T. Chapter 7—The importance of a good night’s sleep. In *A Prescription for Healthy Living*; Academic Press: Cambridge, MA, USA, 2021; pp. 93–102.
2. Chisholm, K.; Ida, K.; Davies, A.; Papkovsky, D.; Singer, M.; Dyson, A.; Tachtsidis, I.; Duchon, M.; Smith, K. In Vivo Imaging of Flavoprotein Fluorescence During Hypoxia Reveals the Importance of Direct Arterial Oxygen Supply to Cerebral Cortex Tissue. *Adv. Exp. Med. Biol.* **2016**, *876*, 233. [[PubMed](#)]
3. Sircan-Kucuksayan, A.; Uyklu, M.; Canpolat, M. Measuring tissue oxygen saturation using NIR spectroscopy. In *Proceedings of the Biophotonics: Photonic Solutions for Better Health Care IV. International Society for Optics and Photonics*; SPIE: Bellingham, WA, USA, 2014; Volume 9129, pp. 369–376.
4. Benjafield, A.; Ayas, N.; Eastwood, P.; Heinzer, R.; Ip, M.; Morrell, M.; Nunez, C.; Patel, S.; Penzel, T.; Pépin, J.L.; et al. Estimation of the global prevalence and burden of obstructive sleep apnoea: A literature-based analysis. *Lancet Respir. Med.* **2019**, *7*, 687–698. [[CrossRef](#)]
5. Ben Simon, E.; Rossi, A.; Harvey, A.; Walker, M. Overanxious and underslept. *Nat. Hum. Behav.* **2020**, *4*, 100–110. [[CrossRef](#)] [[PubMed](#)]
6. Kurth, C.; Levy, W.; Mccann, J. Near-Infrared Spectroscopy Cerebral Oxygen Saturation Thresholds for Hypoxia Ischemia in Piglets. *J. Cereb. Blood Flow Metab.* **2002**, *22*, 335–341. [[CrossRef](#)] [[PubMed](#)]
7. Jöbsis, F. Noninvasive, infrared monitoring of cerebral and myocardial oxygen sufficiency and circulatory parameters. *Science* **1977**, *198*, 1264–1267. [[CrossRef](#)] [[PubMed](#)]
8. Zhu, J.; Mou, J.; Liu, J. Absolute measurement of tissue oxygen saturation with NIRS. In Proceedings of the BIBE 2018 International Conference on Biological Information and Biomedical Engineering, Shanghai, China, 6–8 July 2018; pp. 1–5.
9. Sorensen, L.C.; Leung, T.S.; Greisen, G. Comparison of cerebral oxygen saturation in premature infants by near-infrared spatially resolved spectroscopy: Observations on probe-dependent bias. *J. Biomed. Opt.* **2008**, *13*, 064013. [[CrossRef](#)] [[PubMed](#)]
10. Oniz, A.; Inanc, G.; Taşlıca, S.; Guducu, C.; Ozgoren, M. Sleep Is a Refreshing Process: An fNIRS Study. *Front. Hum. Neurosci.* **2019**, *13*, 160. [[CrossRef](#)] [[PubMed](#)]
11. Nguyen, T.; Babawale, O.; Kim, T.; Jo, H.; Liu, H.; Kim, J. Exploring brain functional connectivity in rest and sleep states: A fNIRS study. *Sci. Rep.* **2018**, *8*, 16144. [[CrossRef](#)] [[PubMed](#)]

12. Ahn, S.; Nguyen, T.; Jang, H.; Kim, J.; Jun, S. Exploring Neuro-Physiological Correlates of Drivers' Mental Fatigue Caused by Sleep Deprivation Using Simultaneous EEG, ECG, and fNIRS Data. *Front. Hum. Neurosci.* **2016**, *10*, 219. [[CrossRef](#)]
13. Marik, Paul, E. Regional carbon dioxide monitoring to assess the adequacy of tissue perfusion. *Curr. Opin. Crit. Care* **2005**, *11*, 245. [[CrossRef](#)]
14. Nagdyman, N.; Ewert, P.; Peters, B.; Miera, O.; Fleck, T.; Schmitt, B. Comparison of different near-infrared spectroscopic cerebral oxygenation indices with central venous and jugular venous oxygenation saturation in children. *Paediatr. Anaesth.* **2008**, *18*, 160–166. [[CrossRef](#)] [[PubMed](#)]
15. Gagnon, R.; Macnab, A.; Gagnon, F.; Blackstock, D.; LeBlanc, J. Comparison of Two Spatially Resolved NIRS Oxygenation Indices. *J. Clin. Monit. Comput.* **2002**, *17*, 385–391. [[CrossRef](#)] [[PubMed](#)]
16. Maswadi, K.; Ghani, N.B.A.; Hamid, S.B. Systematic Literature Review of Smart Home Monitoring Technologies Based on IoT for the Elderly. *IEEE Access* **2020**, *8*, 92244–92261. [[CrossRef](#)]
17. Chance, B.; Zhuang, Z.; UnAh, C.; Alter, C.; Lipton, L. Cognition-activated low-frequency modulation of light absorption in human brain. *Proc. Natl. Acad. Sci. USA* **1993**, *90*, 3770–3774. [[CrossRef](#)] [[PubMed](#)]
18. Duncan, A.; Meek, J.H.; Clemence, M.; Elwell, C.E.; Tyszczyk, L.; Cope, M.; Delpy, D. Optical pathlength measurements on adult head, calf and forearm and the head of the newborn infant using phase resolved optical spectroscopy. *Phys. Med. Biol.* **1995**, *40*, 295–304. [[CrossRef](#)] [[PubMed](#)]
19. Bashkatov, A.; Genina, E.; Tuchin, V. Optical properties of skin, subcutaneous, and muscle tissues: A review. *J. Innov. Opt. Health Sci.* **2011**, *04*, 9–38. [[CrossRef](#)]
20. Sitaram, R.; Zhang, H.; Guan, C.; Thulasidas, M.; Hoshi, Y.; Ishikawa, A.; Shimizu, K.; Birbaumer, N. Temporal classification of multichannel near-infrared spectroscopy signals of motor imagery for developing a brain–computer interface. *NeuroImage* **2007**, *34*, 1416–1427. [[CrossRef](#)] [[PubMed](#)]
21. Everdell, N.; Airantzis, D.; Kolvya, C.; Suzuki, T.; Elwell, C. A portable wireless near-infrared spatially resolved spectroscopy system for use on brain and muscle. *Med. Eng. Phys.* **2013**, *35*, 1692–1697. [[CrossRef](#)] [[PubMed](#)]